npj | Materials Degradation

www.nature.com/npjmatdeg

ARTICLE OPEN

Check for updates

Morphological evolution of Pt-modified nanoporous gold after thermal coarsening in reductive and oxidative environments

A. A. El-Zoka[1]✉, B. Langelier[2], G. A. Botton[2] and R. C. Newman[3]✉

Nanoporous gold made by dealloying AgAuPt (NPG-Pt) has been shown to exhibit several interesting catalytic properties, tied to its exceptionally high surface area; however, structural degradation may occur owing to thermal coarsening. To understand the effect of atmosphere chemistry on thermal coarsening and degradation, and means of limiting it, this study focuses on the high-resolution characterization of NPG-Pt layers coarsened in reductive Ar-H_2 atmosphere, and in oxidative air. Atom probe tomography (APT) analysis is performed on NPG-Pt, coarsened separately in either Ar-H_2 or air, to characterize the atomic-scale chemical changes in the nanoligaments and to develop a mechanistic view of the inherent processes. A tendency of Ag to segregate to the surface during coarsening is found to lead to complete elimination of the nanoligament core-shell structures in both cases. Large Pt segregates form during coarsening in Ar-H_2, but under the surface of the ligaments, having relatively little effect on the coarsening rate. The oxygen-induced segregation of Pt was observed to cause the inhibition of thermal coarsening after minor loss in surface area-to-volume ratio. Findings in this paper help in understanding further the thermal coarsening of heterogeneous nanomaterials made by dealloying, and the pertinent factors that come into play in different chemical environments.

npj Materials Degradation (2020)4:40; https://doi.org/10.1038/s41529-020-00143-4

INTRODUCTION

Nanoporous gold (NPG) is formed by the selective dissolution of Ag from a binary solid solution of Ag and Au[1–3]. Dealloying produces a nanoporous structure, which has a high surface area-to-volume ratio, making it a candidate material for surface area-driven energy applications[4–6]. The functionality of NPG, however, is limited by the stability of its nanostructure, especially if used at elevated temperatures.

NPG-Pt, made from AgAuPt precursors with systematic variation of Pt content, was shown by Vega and Newman to exhibit limited coarsening of ligaments during the dealloying process, making them as small as 3 nm[7]. 3D Atom probe tomography (APT) analysis of the ligaments by the present authors have revealed Pt clustering on nanoligament surfaces, to which the feature size refinement is attributed[8,9]. The use of APT had been considered difficult for NPG and NPG-Pt owing to the high porosity. To address that, a electrodeposition method of Cu was developed to infiltrate the porosity and enable successful APT analysis[10].

NPG-Pt was shown to coarsen significantly in reductive atmospheres, similar to NPG, at temperatures of 250 °C and above[11]. The coarsening of NPG-Pt by Ostwald ripening (OR) eventually leads to the complete annihilation of porosity (i.e., densification), especially when reaching temperatures of 400 °C and above[11]. This is mainly owing to the desegregation of Pt away from the surfaces of nanoligaments as shown by previous studies on Au-Pt nanosystems[12,13].

An interesting property investigated by Vega and Newman in a previous study[14] is that the thermal coarsening of NPG-Pt in air is impeded in the range of 200–500 °C. Oxygen-induced segregation of Pt acts to inhibit the surface diffusion of Au, which is considered as the main facilitator for coarsening to occur at temperatures as low as 200 °C[15]. The favorable interaction of Pt with O (relative to that of Au with O), induces the segregation of Pt atoms to the surface, replacing Au atoms[16].

Changes in the nanoscale chemical composition of as-dealloyed ligaments might not be limited to Pt and Au. Several theoretical studies on Au-Ag nanoparticles have shown the tendency of Ag to segregate to the surface at elevated temperatures[17,18]. Preferential segregation of Ag to the surface was also shown for bulk AgAu alloy[19]. Investigating the changes to chemical and morphological properties of nanoligaments would help in understanding the thermal coarsening process and the functionality of NPG-Pt in reductive and oxidative atmospheres.

The present paper builds upon an atom probe study of dealloying in ternary AgAuPt alloys[8]. In this paper, different behaviors of Au, Ag, and Pt are correlated with the coarsening behavior of NPG-Pt_3 (made from dealloying $AgAuPt_3$) in Ar-H_2 and air at 300 °C, using recently developed APT methods[10] to measure the chemical structure of nanoligaments at the atomic-scale and the associated nanoligament morphologies.

RESULTS AND DISCUSSION

Thermal coarsening in reductive atmosphere

As is clear from the focused ion beam (FIB) cross-section images in Fig. 1c, the ligament sizes for the sample coarsened in the reductive atmosphere are significantly larger (~200 nm) than those observed previously in the APT study of as-dealloyed NPG-Pt_3[8]. Another observation in Fig. 1c, is the voids (dark feature highlighted in inset) present inside the large ligaments. A more recent in situ STEM study of coarsening in reductive atmosphere by the authors[11] showed enclosed voids in NPG and NPG-Pt. Similar voids (or bubbles) were also observed previously using electron tomography[20], and positron annihilation[21]. Kinetic Monte Carlo simulations by Erlebacher[15] alluded to void formation being

[1]Max-Planck-Institut für Eisenforschung GmbH, Max-Planck-Straße 1, Düsseldorf, Germany. [2]Canadian Centre for Electron Microscopy, Department of Materials Science and Engineering, McMaster University, 1280 Main St. W., Hamilton, ON, Canada. [3]Department of Chemical Engineering and Applied Chemistry, University of Toronto, 200 College St., Toronto, ON, Canada. ✉email: a.elzoka@mpie.de; roger.newman@utoronto.ca

Published in partnership with CSCP and USTB

npj nature partner journals

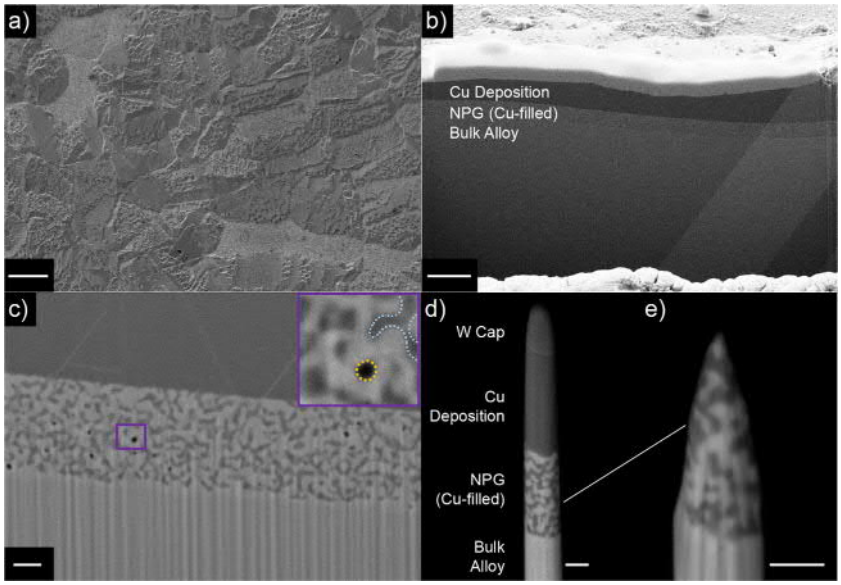

Fig. 1 Cross-sectional analysis and APT specimen preparation of NPG-Pt thermally coarsened in reductive atmosphere. SEM images showing FIB sample preparation of an APT sample for Cu-filled NPG-Pt, heated at 300 °C in Ar-H_2. **a** Sample surface (scale bar is 20 µm). **b** FIB cross-section cut showing the Cu-filled NPG layer, between the Cu deposition and bulk alloy (scale bar is 2 µm). **c** A high magnification image showing the coarsened ligaments and the inset showing an example of entrapped voids (V) within a ligament (L), completely independent from a Cu-filled pore (P) (scale bar is 200 nm). **d** The APT needle following annular milling (scale bar is 200 nm). **e** The final APT specimen after low-kV sharpening (scale bar is 200 nm).

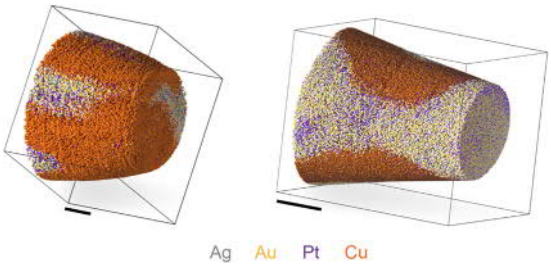

Fig. 2 Atom maps of a single thermally coarsened nanoligament. 3D APT atom maps of Cu-filled NPG-Pt heated at 300 °C in Ar-H_2 showing Au, Ag, Pt, and Cu atoms. Scale bar is 10 nm. Refer to supplementary video for 3D reconstruction.

a result of solid-state Rayleigh instability, controlled by surface diffusion, during coarsening. Although atomistic simulations by Kolluri and Demkowicz[22] suggested that the localized plasticity at nodes and within the ligaments leads to neighboring ligaments collapsing, and ultimately void formation. At this point, the source of these voids and their evolution during thermal coarsening is not yet fully concluded. Future studies focused on microstructural examinations of ligament/pore sizes after dealloying and at successive steps of thermal coarsening should clarify further the source of encased voids, and their role in coarsening.

The shrinkage observed in the nanoporous layer depth owing to coarsening also agrees well with previous measurements, supporting further that shrinkage in the dealloyed layer during thermal coarsening does exist at temperatures where ordinary lattice diffusion is not expected to contribute to the mass transport process. Atom maps for typical samples of NPG-Pt coarsened in Ar-H_2 are shown in Fig. 2, where coarsened ligaments and the surrounding Cu filling are shown.

A chemical profile across a single nanoligament coarsened at 300 °C in reducing atmosphere is presented in Fig. 3. The Ag and Au compositions are both observed to be uniform across the ligament. This result contrasts Ag and Au profiles for as-dealloyed NPG-Pt, as found in previous APT analysis[8–10], which exhibited a clear core-shell structure. As the distribution of Ag and Au is now homogenous, the core-shell structure can be understood as having been eliminated by thermal coarsening. Nanoscale homogenization of originally segregated AgAu nanoparticles was observed previously in reducing environments at elevated temperatures[23]. As for Pt, a clear enrichment towards the core of the ligament, compared with being primarily surface-segregated in the as-dealloyed material, supports the desegregation of Pt from the surface in reductive atmospheres discussed by Vega and Newman[14]. The distribution of Pt is also not as uniform when compared with that of Ag and Au, showing evidence of clustering and segregation from the Ag and Au elements inside the nanoligament.

The surface diffusion dealloying model predicts a Au-rich nanoligament surface owing to the kinetic entrapment of Ag inside ligament cores during their formation[10,24]. More specifically to NPG-Pt, previous APT studies by the authors have observed the co-segregation of Au and Pt at nanoligament surfaces[8]. The current observation, suggesting a tendency of Ag to move to the ligament surface in reductive atmospheres during coarsening, is significant as it shows that Ag contributes to the coarsening process led by diffusion of atoms on nanoligament surfaces. This contribution could be eliminated by increasing the amount of Ag removed during dealloying, as that would decrease further the Ag retained inside nanoligaments by what is known as secondary dealloying[7,25].

The considerable Ag surface enrichment observed at relatively low temperatures for NPG-Pt could be attributed to the role of curvature. A coarsening-mediated Ag surface segregation was shown to have accelerated Ag enrichment at the surface by Pia et al.[26] considering NPG in an environment of CO and O_2.

To monitor the change in Pt distribution across the nanoligaments, chemical mappings across a horizontal 2 nm-thick slice of a few interconnected ligaments are presented in Fig. 4. Large segregates of Pt are observed. In the bigger nanoligament, Pt clusters are located inside the ligaments, consistent with the chemical profile in Fig. 3. Yet other Pt segregates, on the relatively thinner ligaments seem to be at the surfaces. This observation

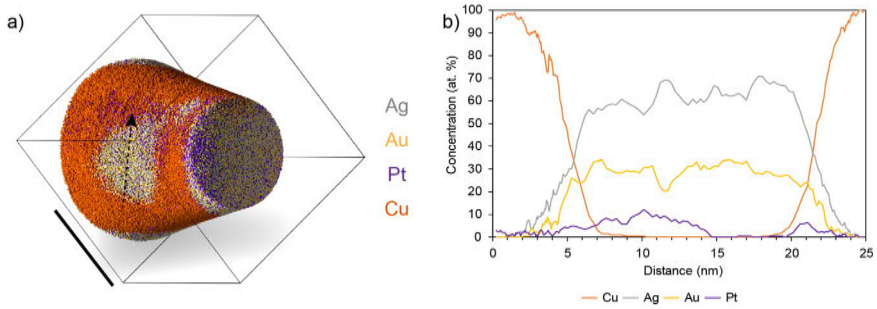

Fig. 3 Elimination of core-shell structure and homogenization of Au-Ag distribution. a APT atom map of a single ligament in a reconstructed volume, showing Au, Ag, Cu atoms. **b** 1D concentration profile through a ligament, as indicated on **a**. Scale bar is 25 nm.

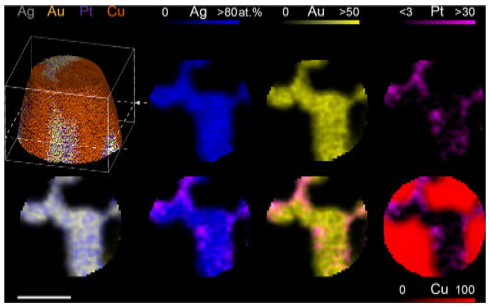

Fig. 4 Formation of subsurface large Pt clusters. Concentration maps taken from 2 nm-thick slices of APT volume of NPG-Pt heated at 300 °C in Ar-H_2. Scale bar is 20 nm.

might appear counterintuitive, as a non-favorable interaction with the reducing atmosphere is expected to drive Pt desegregation from the surface[12,13]. However, considering coarsening kinetics, we postulate that these Pt segregates found at the surfaces of thinner nanoligaments are a result of Pt having a much lower surface mobility than Au[27,28]. This causes the Pt to be left behind at the surfaces of very thin nanoligaments that are shrinking and on the verge of collapsing.

Although it is expected that Pt has a high mobility when moving on a surface of Au[29], it is important to note that Pt is already clustered in as-dealloyed NPG-Pt, making Pt rearrangement even slower[30]. Clusters of several Pt atoms would also have a higher activation energy for moving around as a cluster[31]. Meanwhile, the extremely immobile Pt segregates are increasing in size, due to the tendency to minimize interaction surface area with the reducing atmosphere[32–35], especially at areas of the nanoligaments with high curvature (saddle points)[36].

Inhibited thermal coarsening in oxidative atmosphere

In contrast to NPG-Pt annealed in Ar-H_2, the ligament/pore sizes in the air-annealed NPG-Pt do not show the same coarsening. This can be seen in both the SEM images of the NPG-Pt (Fig. 5) and the APT data (Fig. 6). The cross-sectional image in Fig. 5c reveals a thicker layer of NPG-Pt, compared with H_2-annealed NPG-Pt, and with small feature size, not dissimilar to that observed in as-dealloyed NPG-Pt[9]. This is further supported by a direct comparison of the APT data for the two respective ligament structures, as shown in Fig. 7. Clearly, the thermal coarsening of ligaments was inhibited owing to the oxidative environment, such that the ligament network remains visibly similar in size and scale to the as-dealloyed material.

To understand the effect of the oxidizing environment on the chemical distribution across nanoligaments, chemical mappings are examined. These are shown for a vertical cross-section in Fig. 8. Significant Pt enrichment is observed at ligament surfaces. Compared with the segregates observed in the Ar-H_2-annealed NPG-Pt, the Pt segregates in this case are higher in number, yet considerably smaller. These observations agree with the anticipated adsorbate-induced segregation behavior of Pt which, owing to its favorable interaction with O, is expected to segregate to the ligament surfaces. As a result, Au atom movement on nanoligament surfaces is impeded, leading to mitigated thermal coarsening. Figure 8 also reveals a rather homogenized nanoligament composition, where the as-dealloyed core-shell structure appears to be annealed out. This suggests that while the movement of Au atoms on nanoligament surfaces is impeded due to the high surface area coverage of Pt segregates, the Au (and Ag) atoms within the ligament are sufficiently mobile as to eliminate the non-equilibrium core-shell structure.

A precise indication on the degree of coarsening for NPG-Pt in air is obtained by comparing its measured surface area-to-volume ratio with previously measured values for as-dealloyed NPG-Pt. As shown in Table 1, the volume fraction of the nanoligaments remains basically unchanged by air-annealing. However, a decrease of ~17% in the ligament surface-area-to-volume ratio suggests that some coarsening does occur. It is likely that the coarsening is not totally inhibited until the surfaces of the ligaments are saturated with enough Pt-O clusters to completely immobilize the Au at that temperature.

A final observation made, requiring investigation in future work, is that the total Pt content in the dealloyed layer appeared to increase by as much as 4 at.% after heating in air. Composition profiles from the APT data, excluding Cu, that spans across the dealloying interface are presented in Fig. 9. These show the Pt content increasing moving across the dealloying interface towards the dealloyed layer. This allows us to suggest, for now, that the source of the extra Pt content might be the bulk layer of non-dealloyed $AgAuPt_3$, which could be considered as a reservoir of Pt atoms that, at high enough temperature, could diffuse across the non-uniform dealloying interface.

Diffusion across the dealloying interface at 300 °C, where minimal lattice diffusion is expected, could be assisted by excessive point defects[37] injected at the dealloying front, as per previous discussions on the topic by Rösner and Weissmüller[20]. Nevertheless, this is yet to be validated through future in-depth studies that could reveal an interesting substrate effect on the functionality of NPG-Pt at high temperatures.

The findings presented in this paper highlight the different roles played by Ag, Au, and Pt during thermal coarsening and how such roles are closely dependent on chemical environment of coarsening. In reducing environments, nanoligaments increase in size due to the surface diffusion of Au. Ag segregates to nanoligament surfaces, highlighting the possible contribution of Ag to the coarsening of nanoligaments in nanoporous layers with residual Ag. Meanwhile, large clusters of Pt are formed on subsurfaces of coarsened ligament. Nanoligaments on the verge

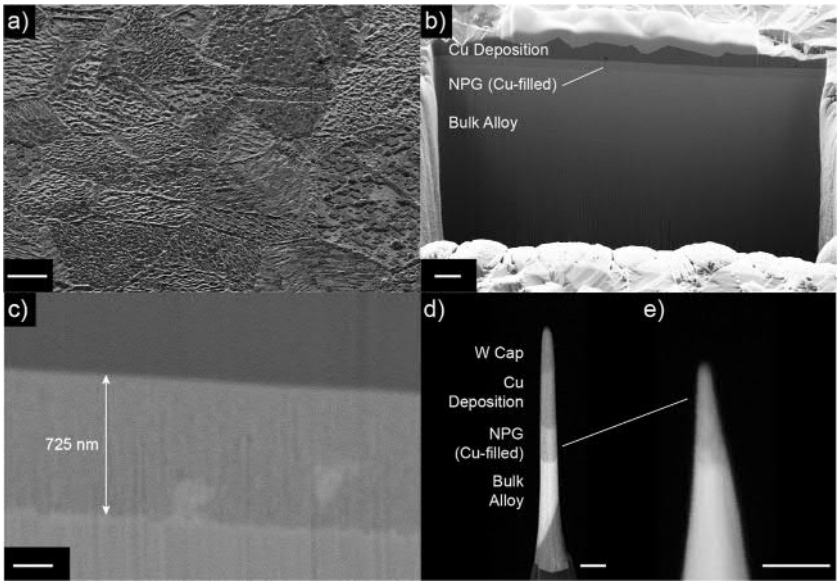

Fig. 5 Cross-sectional analysis and APT specimen preparation of NPG-Pt thermally coarsened in oxidative atmosphere. SEM images showing FIB sample preparation of an APT sample for Cu-filled NPG-Pt, heated at 300 °C in air. **a** Sample surface (scale bar is 20 µm). **b** Cut out showing the Cu-filled NPG layer, between the Cu deposition and bulk alloy (scale bar is 2 µm). **c** A high magnification image showing the fine ligament-pore structure (scale bar is 200 nm). **d** The APT needle following annular milling (scale bar is 500 nm). **e** The final APT specimen after low-kV sharpening (scale bar is 200 nm).

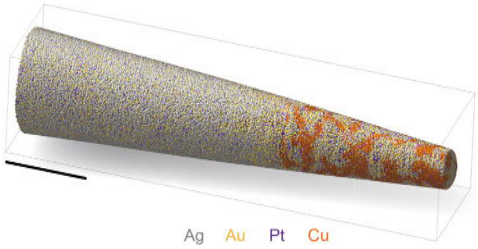

Fig. 6 Atom map of NPG-Pt layer along with the parent alloy (AgAuPt) after coarsening in air. 3D APT atom maps of Cu-filled dealloyed layer on NPG-Pt, air-annealed at 300 °C for 2 h showing Au, Ag, Pt, and Cu atoms. Scale bar is 50 nm. Refer to supplementary video for 3D reconstruction.

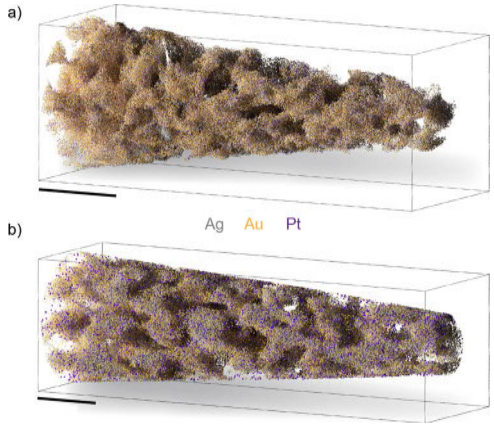

Fig. 7 Retained ligament-pore structure in NPG-Pt after annealing in air, owing to impeded thermal coarsening. a 3D atom maps showing ligaments of **a** NPG-Pt air-annealed at 300 °C for 2 h, and **b** as-dealloyed NPG-Pt (full methodology for spatially-determining the ligament boundaries and data for as-dealloyed NPG-Pt from ref. [8]). Scale bar is 20 nm.

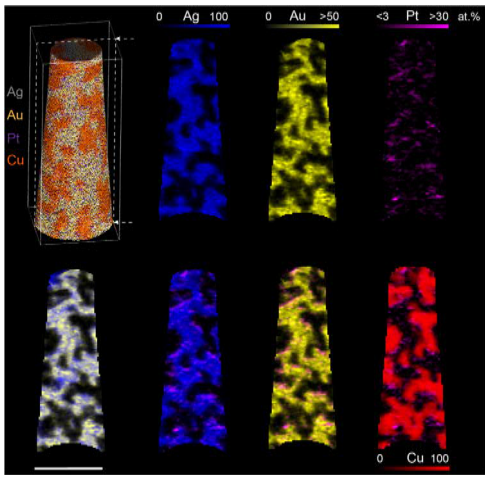

Fig. 8 Formation of nanoscale Pt surface segregates and elimination of core-shell distribution of AgAu. Concentration maps taken from 5 nm-thick slices of APT volumes of NPG-Pt air-annealed at 300 °C for 2 h, along the longitudinal axis. Scale bar is 30 nm.

of collapsing had immobile Pt segregates at the surface, left behind by the more mobile Ag and Au.

In oxidative environments, thermal coarsening is inhibited owing to the enrichment of Pt at nanoligament surfaces, via the positive interaction between O and Pt. The nanoligament size showed little change as a result. The core-shell structure of as-dealloyed ligaments is also eliminated in oxidative air, even though the change in surface area-to-volume ratio is minimal and surface diffusion of Ag, Au is practically inhibited. Compositional changes across the entire dealloyed layer remain to be further investigated, with particular focus on local chemistry at the dealloying interface.

Table 1. Limited degradation of surface area-to-volume ratio after annealing in oxidative environment.

	Volume fraction NPG	Surface area NPG/NPG volume (nm^{-1})
NPG-$AuAgPt_3$ (annealed in air)	0.501	0.479
NPG-$AuAgPt_3$	0.520	0.576

Volume fractions, and ratios of surface area-to-volume for NPG-Pt annealed in air, and as-dealloyed NPG, obtained by APT (full methodology and data for as-dealloyed NPG-Pt from ref. [8]).

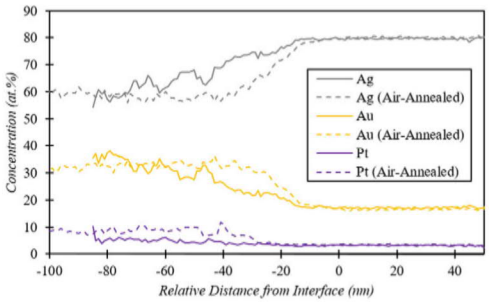

Fig. 9 Overall Pt enrichment in NPG-Pt after coarsening in air. 1D concentration profiles for NPG-Pt air-annealed at 300 °C for 2 h and as-dealloyed NPG crossing the dealloying interface.

METHODS

Dealloying

Two rectangular samples with nominal surface areas of ~0.8 cm^2 were cut out of 200 µm foil of $Ag_{77}Au_{20}Pt_3$ (at.%) procured from Goodfellow Metals, Cambridge, UK. All annealing was done at 975 °C for 15 h in a 2.5% H_2-Ar atmosphere. The samples were then soldered to a copper electrical wire from one end (taking care not to alter the active surface area to be dealloyed). A fine coating of Microshield ™ lacquer supplied by SPI was applied to the solder-copper-sample junction to insulate it from the solution used. Dealloying solution was prepared with 18 MΩ cm de-ionized water and de-aerated by high-purity N_2 purging (min purity: 99.998%). The samples were then dealloyed potentiostatically, at room temperature, in a solution of 0.5 M $HClO_4$ from Analar grade $HClO_4$ (Alfa-Aesar, 62%), at a potential of 550 mV vs. MSE (Mercury/Mercurous Sulfate Electrode/sat. K_2SO_4), until the removal of ~0.5 C cm^{-2} was attained. The dealloyed samples were then immersed in de-ionized water for ~1 h to remove residual acid.

After cutting the NPG-Pt samples to detach them from the lacquered wire, they were annealed in two separate conditions, one for 2 h in a reducing atmosphere of Ar-2.5% H_2 at 300 °C followed by quenching in furnace by purging Ar-2.5% H_2, and the other for 2 h in oxidizing laboratory air at 300 °C followed by air quenching. Then the annealed samples were reattached to a copper electrical wire from one end and coated with an insulating layer of lacquer, as explained above, for pore infiltration by Cu deposition. Pore infiltration was then achieved by stepped potentiostatic deposition of Cu in $CuSO_4 + H_2SO_4$ solution, following the deposition method explained in a previous APT analysis published recently[10].

Atom probe tomography

APT samples were prepared from the Cu-filled dealloyed layer of NPG-Pt_3 using a Zeiss NVision40 FIB and standard liftout procedures[38]. Target areas in the sample, with well-filled dealloyed layers, were identified by cross-sectional FIB cuts, and then extracted with a micro-manipulator. Specimens were then mounted to pre-sharpened Si posts using deposition of W. The samples were then sharpened into needles of suitable scale for APT using the FIB. Initial annular milling was conducted at 30 kV, with final cleaning/sharpening at 10 kV.

APT analysis was conducted using a Cameca local electrode atom probe (LEAP) ×4000 HR (Cameca Instruments, USA). Data were acquired while operating in laser-pulsing mode ($\lambda = 355$ nm) with a pulse of 40–60 pJ and a pulse rate of 100–125 kHz. The target evaporation rate was set to 0.003 or 0.005 ions per pulse (0.3 or 0.5%) by adjusting an applied DC voltage (typically ranging from ~2 to 5 kV). The base temperature for the specimen stage during analysis was ~60 K, and the chamber pressure was approximately 10^{-8} Pa. Reconstruction and analysis were performed using IVAS 3.8 software, using SEM images of the tips to assist with spatial calibration of the reconstructions.

DATA AVAILABILITY

The data that support the findings of this study are available from the corresponding authors upon request.

Received: 2 July 2020; Accepted: 31 October 2020;
Published online: 07 December 2020

REFERENCES

1. Newman, R. C. 2.05–Dealloying. In *Shreir's Corrosion* (eds. Cottis, B. et al.) 801–809 (Elsevier, 2010).
2. Erlebacher, J., Newman, R. C. & Sieradzki, K. Fundamental Physics and Chemistry of Nanoporosity Evolution During Dealloying. In *Nanoporous Gold: From an Ancient Technology to a High-Tech Material* 11–29 (2012).
3. Erlebacher, J. & Sieradzki, K. Pattern formation during dealloying. *Scr. Mater.* **49**, 991–996 (2003).
4. Zugic, B. et al. Dynamic restructuring drives catalytic activity on nanoporous gold-silver alloy catalysts. *Nat. Mater.* **16**, 558–564 (2017).
5. Villani, E. et al. Coreactant electrochemiluminescence at nanoporous gold electrodes. *Electrochim. Acta* **277**, 168–175 (2018).
6. Vega, A. A. & Newman, R. C. Methanol electro-oxidation on nanoporous metals formed by dealloying of Ag–Au–Pt alloys. *J. Appl. Electrochem.* **46**, 995–1010 (2016).
7. Vega, A. A. & Newman, R. C. Nanoporous metals fabricated through electrochemical dealloying of Ag-Au-Pt with systematic variation of Au:Pt ratio. *J. Electrochem. Soc.* **161**, C1–C10 (2014).
8. El-Zoka, A. A., Langelier, B., Korinek, A., Botton, G. A. & Newman, R. C. Nanoscale mechanism of the stabilization of nanoporous gold by alloyed platinum. *Nanoscale* **10**, 4904–4912 (2018).
9. El-Zoka, A. A., Langelier, B., Korinek, A., Botton, G. A. & Newman, R. C. Advances in nanoscale characterization of refined nanoporous gold. *Electrochim. Acta* **283**, https://doi.org/10.1016/j.electacta.2018.06.198 (2018).
10. El-Zoka, A. A., Langelier, B., Botton, G. A. & Newman, R. C. Enhanced analysis of nanoporous gold by atom probe tomography. *Mater. Charact.* **128**, 269–277 (2017).
11. El-Zoka, A. A., Howe, J. Y., Newman, R. C. & Perovic, D. D. In situ STEM/SEM study of the coarsening of nanoporous gold. *Acta Mater.* **162**, 67–77 (2019).
12. Wanjala, B. N., Luo, J., Fang, B., Mott, D. & Zhong, C. J. Gold-platinum nanoparticles: alloying and phase segregation. *J. Mater. Chem.* **21**, 4012–4020 (2011).
13. Ruban, A. V., Skriver, H. L. & Nørskov, J. K. Surface segregation energies in transition-metal alloys. *Phys. Rev. B* **59**, 15990–16000 (1999).
14. Vega, A. A. & Newman, R. C. Beneficial effects of adsorbate-induced surface segregation of Pt in nanoporous metals fabricated by dealloying of Ag-Au-Pt alloys. *J. Electrochem. Soc.* **161**, C11–C19 (2014).
15. Erlebacher, J. Mechanism of coarsening and bubble formation in high-genus nanoporous metals. *Phys. Rev. Lett.* **106**, 225504 (2011).
16. Dhouib, A. & Guesmi, H. DFT study of the M segregation on MAu alloys (M = Ni, Pd, Pt) in presence of adsorbed oxygen O and O2. *Chem. Phys. Lett.* **521**, 98–103 (2012).
17. Deng, L., Hu, W., Deng, H., Xiao, S. & Tang, J. Au-Ag bimetallic nanoparticles: surface segregation and atomic-scale structure. *J. Phys. Chem. C.* **115**, 11355–11363 (2011).
18. Negreiros, F. R., Soares, E. A., De Carvalho, V. E. & Bozzolo, G. Atomistic modeling of Au-Ag nanoparticle formation. *Phys. Rev. B* **76**, 245432 (2007).
19. Van Santen, R. A. & Boersma, M. A. M. Theory of surface enrichment in disordered monophasic binary alloys. Numerical computations for Ag-Au alloys. *J. Catal.* **34**, 13–18 (1974).
20. Rösner, H., Parida, S., Kramer, D., Volkert, C. A. & Weissmüller, J. Reconstructing a nanoporous metal in three dimensions: An electron tomography study of dealloyed gold leaf. *Adv. Eng. Mater.* **9**, 535–541 (2007).
21. Viswanath, R. N., Chirayath, V. A., Rajaraman, R., Amarendra, G. & Sundar, C. S. Ligament coarsening in nanoporous gold: Insights from positron annihilation study. *Appl. Phys. Lett.* **102**, 253101 (2013).

22. Kolluri, K. & Demkowicz, M. J. Coarsening by network restructuring in model nanoporous gold. *Acta Mater.* **59**, 7645–7653 (2011).
23. Yen, C. W. et al. CO oxidation catalyzed by Au-Ag bimetallic nanoparticles supported in mesoporous silica. *J. Phys. Chem. C.* **113**, 17831–17839 (2009).
24. Liu, Y., Bliznakov, S. & Dimitrov, N. Factors controlling the less noble metal retention in nanoporous structures processed by electrochemical dealloying. *J. Electrochem. Soc.* **157**, K168–K176 (2010).
25. Ye, X.-L. et al. Primary and secondary dealloying of Au(Pt)-Ag: structural and compositional evolutions, and volume shrinkage. *J. Electrochem. Soc.* **161**, C517–C526 (2014).
26. Pia, G., Sogne, E., Falqui, A. & Delogu, F. Ag surface segregation in nanoporous Au catalysts during CO oxidation. *Sci. Rep.* **8**, 15208 (2018).
27. Göbel, H. & von Blanckenhagen, P. A study of surface diffusion on gold with an atomic force microscope. *Surf. Sci.* **331–333**, 885–890 (1995).
28. Lin, T. S. & Chung, Y. W. Measurement of the activation energy for surface diffusion in gold by scanning tunneling microscopy. *Surf. Sci.* **207**, 539–546 (1989).
29. Leppert, L., Albuquerque, R. Q. & Foster, A. S. & Kümmel, S. Interplay of electronic structure and atomic mobility in nanoalloys of au and pt. *J. Phys. Chem. C.* **117**, 17268–17273 (2013).
30. Deák, R., Néda, Z. & Barna, P. B. A kinetic Monte Carlo approach for self-diffusion of Pt atom clusters on a Pt(111) surface. *Commun. Comput. Phys.* **10**, 920–939 (2011).
31. Liu, S., Zhang, Z., Nørskov, J. & Metiu, H. The mobility of Pt atoms and small Pt clusters on Pt(111) and its implications for the early stages of epitaxial growth. *Surf. Sci.* **321**, 161–171 (1994).
32. Schoeb, A. M. et al. Driving force for surface segregation in bimetallic catalysts. *Surf. Sci.* **278**, L125–L130 (1992).
33. Zhou, C. et al. Growth pathway of Pt clusters on α-Al2O3(0001) surface. *J. Phys. Chem. C.* **111**, 13786–13793 (2007).
34. Oudenhuijzen, M. K., Bitter, J. H. & Koningsberger, D. C. The nature of the Pt-H bonding for strongly and weakly bonded hydrogen on platinum. A XAFS spectroscopy study of the Pt-H antibonding shaperesonance and Pt-H EXAFS. *J. Phys. Chem. B* **105**, 4616–4622 (2001).
35. Stephan, J. J., Ponec, V. & Sachtler, W. M. H. The temperature programmed desorption of hydrogen from platinum and platinum-gold films. *Surf. Sci.* **47**, 403–412 (1975).
36. Fujita, T. et al. Atomic origins of the high catalytic activity of nanoporous gold. *Nat. Mater.* **11**, 775–780 (2012).
37. Schumacher, D., Seeger, A. & Härlin, O. Vacancies, divacancies, and self-diffusion in platinum. *Phys. Status Solidi* **25**, 359–371 (1968).
38. Thompson, K. et al. In situ site-specific specimen preparation for atom probe tomography. *Ultramicroscopy* **107**, 131–139 (2007).

ACKNOWLEDGEMENTS

The authors acknowledge support by an NSERC Discovery Grant (RGPIN-2014-03995) and Accelerator Supplement (RGPAS 462039-14) awarded to R.C. Newman. The authors acknowledge the facilities, scientific, and technical assistance from the Canadian Centre for Electron Microscopy (CCEM) a facility supported by the Canada Foundation for Innovation under the Major Science Initiative program, NSERC and at McMaster University.

AUTHOR CONTRIBUTIONS

A.E. and R.C.N. designed the research. A.E. carried out the dealloying, heat treatment, and inner-pore electrodeposition. B.L. carried out the FIB sample preparation and APT experiments. B.L., G.B., A.E., R.C.N. analyzed the APT data. A.E. lead the writing of the manuscript. All authors contributed to the editing of the paper, and approval of the content in its current form.

FUNDING

Open Access funding enabled and organized by Projekt DEAL.

COMPETING INTERESTS

The authors declare no competing interests.

ADDITIONAL INFORMATION

Supplementary information is available for this paper at https://doi.org/10.1038/s41529-020-00143-4.

Correspondence and requests for materials should be addressed to A.A.E.-Z. or R.C.N.

Reprints and permission information is available at http://www.nature.com/reprints

Publisher's note Springer Nature remains neutral with regard to jurisdictional claims in published maps and institutional affiliations.